

Convective Heat and Mass Transfer Flow of Siskonanofluid Past a Nonlinear Stretching Sheet with Thermal Radiation

G.Venkata Ramanaiyah¹, Dr.M.Sreedhar Babu², M.Lavanya³

¹Research scholar, Dept. of Applied Mathematics, Y.V.University, Kadapa Andhra Pradesh, India.
Cell no:9885229604

²Asst.professor, Dept. of Applied Mathematics, Y.V.University, Kadapa Andhra Pradesh, India.
Cell no: 9959656072.

³Research scholar, Dept. of Applied Mathematics, Y.V.University, Kadapa Andhra Pradesh, India.
Cell no :9494218601.

Abstract:- The steady two-dimensional flow of a Siskonanofluid over a non-linear stretching surface in the presence of thermal radiation and convective boundary condition is investigated. Similarity transformations are employed to transform the governing partial differential equations into ordinary differential equations. The transformed equations are then solved numerically by Bvp4c Matlab solver. The flow features and heat and mass transfer characteristics for different values of the governing parameters viz. thermophoresis parameter, Brownian motion parameter, thermal radiation parameter, Prandtl number, material parameter, thermal Biot number, Lewis number and concentration Biot number are analyzed and discussed in detail. The local Nusselt number increases with increases the thermal Biot number whereas local Nusselt number decreases with an increase the concentration Biot number. The local Sherwood number increases with increases the concentration Biot number whereas local Sherwood number decreases with an increase the thermal Biot number.

Keywords:- Siskonanofluid, Convective Heat and Mass Transfer, non-linear Stretching Sheet.

I. INTRODUCTION

Nanotechnology has immense applications in industry since materials with sizes of nanometers exhibit unique physical and chemical properties. Fluids with nano-scaled particles interaction are called nanofluid. It represents the most relevant technological cutting edge currently being explored. Nanofluid heat transfer is an innovative technology which can be used to enhance heat transfer. Nanofluid is a suspension of solid nanoparticles (1–100nm diameters) in conventional liquids like water, oil, and ethylene glycol. Depending on shape, size, and thermal properties of the solid nanoparticles, the thermal conductivity can be increased by about 40% with low concentration (1%–5% by volume) of solid nanoparticles in the mixture. The nanoparticles used in nanofluid are normally composed of metals, oxides, carbides, or carbon nanotubes. Water, ethylene glycol, and oil are common examples of base fluids. Nanofluids have their major applications in heat transfer, including microelectronics, fuel cells, pharmaceutical processes, and hybrid-powered engines, domestic refrigerator, chiller, nuclear reactor coolant, grinding, space technology, and boiler flue gas temperature reduction. They demonstrate enhanced thermal conductivity and convective heat transfer coefficient counterbalanced to the base fluid. Nanofluids have been the core of attention of many researchers for new production of heat transfer fluids in heat exchangers, plants, and automotive cooling significations, due to their enormous thermal characteristics, Nadeem et al. [1]. The nanofluid is stable; it introduces very little pressure drop, and it can pass through nanochannels (e.g., see Zhou [2]). The word nanofluid was coined by Choi [3]. Xuan and Li [4] pointed out that, at higher nanoparticle volume fractions, the viscosity increases sharply, which suppresses heat transfer enhancement in the nanofluid. Therefore, it is important to carefully select the proper nanoparticle volume fraction to achieve heat transfer enhancement. Buongiorno noted that the nanoparticles' absolute velocity can be viewed as the sum of the base fluid velocity and a relative velocity (which he called the slip velocity). He considered in turn seven slip mechanisms: inertia, Brownian diffusion, thermophoresis, diffusiophoresis, Magnus effect, fluid drainage, and gravity settling.

In recent years, investigations on the boundary layer flow problem with a convective surface boundary condition have gained much interest among researchers, since first introduced by Aziz [5], who considered the thermal boundary layer flow over a flat plate in a uniform free stream with a convective surface boundary condition. This problem was then extended by Bataller [6] by considering the Blasius and Sakiadis flows, both under a convective surface boundary condition and in the presence of thermal radiation. Ishak [7] obtained the similarity solutions for the steady laminar boundary layer flow over a permeable plate with a convective boundary condition. Makinde and Aziz [8] investigated numerically the effect of a convective boundary condition on the two dimensional boundary layer flows past a stretching sheet in a nanofluid. Boundary Layer

Flow over a Stretching Sheet with a Convective Boundary Condition and Slip Effect has studied by Nor Ashikin Abu Bakar et al [9]. Soret and Dufour effects on hydro magnetic Heat and Mass Transfer over a Vertical Plate with a Convective Surface Boundary Condition and Chemical reaction were studied byGangadhar [10].

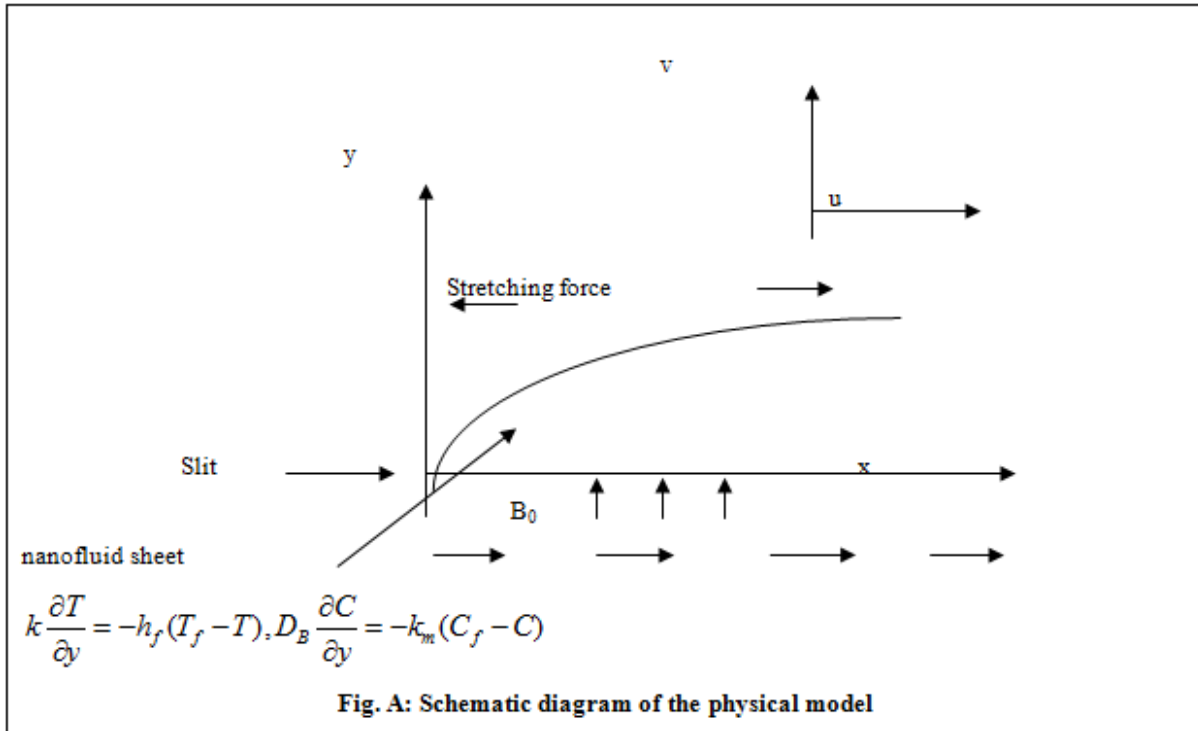
In the context of space technology and in processes involving high temperatures, the effects of radiation are of vital importance. Studies of free convection flow along a vertical cylinder or horizontal cylinder are important in the field of geothermal power generation and drilling operations where the free stream and buoyancy induced fluid velocities are of roughly the same order of magnitude. Many researchers such as Arpaci [11], Cess [12], Cheng and Ozisik [13], Raptis [14], Hossain and Takhar [15, 16] have investigated the interaction of thermal radiation and free convection for different geometries, by considering the flow to be steady. Oahimire et al.[17] studied the analytical solution to mhdmicropolar fluid flow past a vertical plate in a slip-flow regime in the presence of thermal diffusion and thermal radiation. El-Arabawy [18] studied the effect of suction/injection on a micropolar fluid past a continuously moving plate in the presence of radiation. Ogulu [19] studied the oscillating plate-temperature flow of a polar fluid past a vertical porous plate in the presence of couple stresses and radiation. Mat et al. [20] studied the radiation effect on marangoni convection boundary layer flow of a nanofluid.Khan et al. [21] considered the MHD radiative, heat-generating and chemical reacting nanofluid flow past a wedge and concluded that with increasing independently thermal convective parameter and radiation than temperature increased significantly, whereas the opposite effect has been found for mass convective (species buoyancy) and heat generation parameter respectively.

Madhu and Kishan [22] studied the influence of Brownian motion and thermophoresis on mixed convection magneto hydrodynamic boundary layer flow of heat and mass transfer stagnation-point flow of power-law non-Newtonian nanofluid towards a stretching surface and concluded that effect of Brownian motion Nb is to increase the temperature profiles and decrease the concentration profiles. Kameswaran and Precious Sibanda [23] investigated the effects of thermal dispersion on non-Newtonian power-law nanofluid flow over an impermeable vertical plate and used a mathematical model for the nanofluid that incorporates the effects of nanoparticle Brownian motion and thermophoresis. Yacob&Ishak [24] investigated the two-dimensional laminar flow of a power-law fluid over a permeable shrinking sheet of constant surface temperature. Hayatetal. [25] studied the effect of Newtonian heating in the laminar flow of power law nanofluid. Das et al. [26] investigated the heat and mass transfer of an electrically conducting incompressible nanofluid over a heated stretching sheet with convective boundary condition and concluded that an increase in the surface convection parameter, thermal radiation parameter, Brownian motion parameter and thermophoretic parameter lead to an increase in the thermal boundary layer thickness. Hayat et al. [27] numerically investigated the effects of convective heat and mass transfer in the flow of Powell-Erying fluid past an inclined exponential stretching surface with Soret and Dufour effects. Rashidi et al. [28] investigated the MHD heat and mass transfer flow of a steady viscous incompressible fluid over a flat plate with convective surface boundary conditions by using the one parameter continuous group method and concluded the thickness of the thermal boundary layer increases with an increase in thermal conductivity parameter. Kandasamy et al. [29] investigated the influence of thermophoresis, Brownian motion of the nanoparticles with variable stream conditions in the presence of magnetic field on mixed convection heat and mass transfer in the boundary layer region of a semi-infinite porous vertical plate in a nanofluid under the convective boundary conditions. Khan et al. [30] investigated the two-dimensional boundary layer flow and heat transfer to Siskonanofluid over a nonlinearly stretching sheet. Khan and Pop [31] investigated the boundary-layer flow of a nanofluid past a stretching sheet.Nandy et al.[32] investigated the forced convection in unsteady boundary layer flow of nanofluid over a permeable shrinking sheet in the presence of thermal radiation.

However, the interactions of the steady flow of a Siskonanofluid over a non-linear stretching surface in the presence of thermal radiation and convective boundary condition is considered.The governing boundary layer equations have been transformed to a two-point boundary value problem in similarity variables and the resultant problem is solved numerically using bvp4c MATLAB solver. The effects of various governing parameters on the fluid velocity, temperature, concentration, the rate of heat and mass transfer are shown in figures and analyzed in detail.

II. MATHEMATICAL FORMULATION

Consider the laminar, two-dimensional, steady flow and heat transfer of the Siskonanofluid in the region $y > 0$ driven by a sheet stretching with power-law velocity $U = cx^s$, where c represents a non-negative real number and $s > 0$ represents the stretching rate of the sheet. Schematic diagram of the physical model is shown in figure A.



The stretching sheet is assumed to be coinciding with the x – axes while the y - axis is perpendicular to the plane of the sheet. A hot fluid with temperature T_f is utilized to heat up or cool down the surface of the sheet (to be determined later) by convective heat transfer mode, which provides the heat transfer coefficient h_f and convective concentration near the surface is C_f with k_m is the wall mass transfer coefficient. We assume the uniform nanoparticle volume fraction of the surface of the stretching sheet is C_w , whereas the ambient temperature and nanoparticle volume fraction are T_∞ and C_∞ , respectively.

The governing equations of motion, the energy and mass equation may be written in usual notation as Continuity equation

$$\frac{\partial u}{\partial x} + \frac{\partial v}{\partial y} = 0 \quad (2.1)$$

Momentum equation

$$u \frac{\partial u}{\partial x} + v \frac{\partial u}{\partial y} = \frac{a}{\rho} \frac{\partial^2 u}{\partial y^2} - \frac{b}{\rho} \frac{\partial}{\partial y} \left(-\frac{\partial u}{\partial y} \right)^n \quad (2.2)$$

Energy equation

$$u \frac{\partial T}{\partial x} + v \frac{\partial T}{\partial y} = \alpha \frac{\partial^2 T}{\partial y^2} - \frac{1}{\rho c_p} \frac{\partial q_r}{\partial y} + \tau \left[D_B \frac{\partial C}{\partial y} \frac{\partial T}{\partial y} + \frac{D_T}{T_\infty} \left(\frac{\partial T}{\partial y} \right)^2 \right] \quad (2.3)$$

Spices equation

$$u \frac{\partial C}{\partial x} + v \frac{\partial C}{\partial y} = D_B \frac{\partial^2 C}{\partial y^2} + \frac{D_T}{T_\infty} \frac{\partial^2 T}{\partial y^2} \quad (2.4)$$

The boundary conditions are

$$\begin{aligned}
 u(x, y) = U = cx^s, v(x, y) = 0, k \frac{\partial T(x, y)}{\partial y} = -h_f (T_f - T(x, y)) \\
 D_B \frac{\partial C(x, y)}{\partial y} = -k_m (C_f - C(x, y)) \\
 u \rightarrow 0, T \rightarrow T_\infty, C \rightarrow C_\infty \text{ as } y \rightarrow \infty
 \end{aligned}
 \tag{2.5}$$

Here u and v denote the components of velocity along x - and y - axes respectively, a, b and n ($n \geq 0$) are the material constants of the Sisko fluid, T and C represent the temperature and solid nanoparticle volume fraction, ρ, σ, α ($= k / (\rho c_p)_f$) and k represent the fluid density, electrical conductivity, q_r is the radiative heat flux, thermal diffusivity and thermal conductivity. Furthermore, τ ($= (\rho c)_p / (\rho c)_f$) represents the ratio of effective heat capacity of the nanoparticle material (i.e., $(\rho c)_p$) to the heat capacity of the fluid (i.e., $(\rho c)_f$), D_B and D_T represent the Brownian diffusion coefficient and thermophoresis diffusion coefficient, respectively.

By using the Rosseland approximation the radiative heat flux q_r is given by

$$q_r = -\frac{4\sigma^*}{3k^*} \frac{\partial T^4}{\partial y}
 \tag{2.6}$$

Where σ^* is the Stefan -Boltzmann constant and k^* is the mean absorption coefficient. It should be noted that by using the Rosseland approximation, the present analysis is limited to optically thick fluids. If temperature differences within the flow are significantly small, then equation (2.6) can be linearised by expanding T^4 into the Taylor series about T_∞ , which after neglect higher order terms takes the form:

$$T^4 \cong 4T_\infty^3 T - 3T_\infty^4
 \tag{2.7}$$

In view of equations (2.6) and (2.7), eqn. (2.3) reduces to

$$u \frac{\partial T}{\partial x} + v \frac{\partial T}{\partial y} = \left(\alpha + \frac{16\sigma^* T_\infty^3}{3k^* \rho c_p} \right) \frac{\partial^2 T}{\partial y^2} + \tau \left[D_B \frac{\partial C}{\partial y} \frac{\partial T}{\partial y} + \frac{D_T}{T_\infty} \left(\frac{\partial T}{\partial y} \right)^2 \right]
 \tag{2.8}$$

Introducing the non-dimensional variables and quantities as

$$\begin{aligned}
 \eta = \frac{y}{x} \text{Re}_b^{\frac{1}{n+1}}, f' = \frac{u}{U}, \theta = \frac{T - T_\infty}{T_f - T_\infty}, \phi = \frac{C - C_\infty}{C_f - C_\infty}, u(x, y) = Uf'(\eta), \\
 v(x, y) = -U \text{Re}_b^{-\frac{1}{n+1}} \frac{1}{n+1} \left[\{s(2n-1)+1\} f(\eta) + \{s(2-n)-1\} \eta f'(\eta) \right] \\
 \text{Re}_a = \frac{\rho x U}{a}, \text{Re}_b = \frac{\rho x^n U^{2-n}}{b}, A = \frac{\text{Re}_b^{2/n+1}}{\text{Re}_a}, \text{Pr} = \frac{x U}{\alpha} \text{Re}_b^{\frac{-2}{n+1}}, \text{Bi}_1 = \frac{h_f}{k} x \text{Re}_b^{\frac{-1}{n+1}} \\
 \text{Nb} = \frac{\tau D_B (C_f - C_\infty)}{\alpha}, \text{Nt} = \frac{\tau D_T (T_f - T_\infty)}{T_\infty \alpha}, \text{Le} = \frac{\alpha}{D_B}, \text{Bi}_1 = \frac{k_m}{D_B} x \text{Re}_b^{\frac{-1}{n+1}}, \\
 R = \frac{16\sigma^* T_\infty^3}{3k^* \alpha \rho c_p}
 \end{aligned}
 \tag{2.9}$$

where $f(\eta)$ is the dimensionless stream function, $\theta(\eta)$ is the dimensionless temperature, $\phi(\eta)$ is the dimensionless concentration, η is the similarity variable, Re_a and Re_b is the local Reynolds numbers, A is the material parameter of the Sisko fluid, Pr is the generalized Prandtl number, Bi_1 is the generalized thermal Biot number with $\text{Bi}_1 \rightarrow \infty$, the thermal convective boundary condition reduces to the uniform surface temperature boundary condition, Nb is the Brownian motion parameter, Nt is the thermophoresis parameter, Le

is the Lewis number, Bi_2 is the generalized concentration Biot number with $Bi_2 \rightarrow \infty$, the concentration convective boundary condition reduces to the uniform surface concentration boundary condition, R is the thermal radiation parameter.

Substituting equations (2.9) in (2.2), (2.4) and (2.8), we have

$$Af''' + n(-f'')^{n-1} f''' + \left(\frac{s(2n-1)+1}{n+1} \right) f f'' - s f'^2 = 0 \tag{2.10}$$

$$\left(\frac{1}{1+R} \right) \theta'' + Pr \left(\frac{s(2n-1)+1}{n+1} \right) f \theta' + Nb \theta' \phi' + Nt \theta'^2 = 0 \tag{2.11}$$

$$\phi'' + Pr Le \left(\frac{s(2n-1)+1}{n+1} \right) f \phi' + \frac{Nt}{Nb} \theta'' = 0 \tag{2.12}$$

The transformed boundary conditions can be written as

$$f(0) = 0, f'(0) = 1, \theta'(0) = -Bi_1 [1 - \theta(0)], \phi'(0) = -Bi_2 [1 - \phi(0)] \\ f' \rightarrow 0, \theta \rightarrow 0, \phi \rightarrow 0 \text{ as } \eta \rightarrow \infty \tag{2.13}$$

where primes denote differentiation with respect to η

The physical quantities of interest are the wall skin friction coefficient C_{fx} , the local Nusselt number Nu_x and the local Shearwood number Sh_x which are defined as

$$C_{fx} = \frac{\tau_{xy}|_{y=0}}{\frac{1}{2} \rho U^2}, Nu_x = \frac{xq_w|_{y=0}}{\alpha(T_f - T_\infty)}, Sh_x = \frac{xj_w|_{y=0}}{D_B(C_f - C_\infty)} \tag{2.14}$$

where τ_{xy} is the shear stress or skin friction along the stretching sheet, q_w is the heat flux from the sheet and j_w is the mass flux from the sheet and those are defined as

$$\tau_{xy} = \left(a + b \left| \frac{\partial u}{\partial y} \right|^{n-1} \right) \left(\frac{\partial u}{\partial y} \right) \\ q_w = -\alpha \left(\frac{\partial T}{\partial y} \right) \\ j_w = -D_B \left(\frac{\partial C}{\partial y} \right) \tag{2.15}$$

Thus, we get the wall skin friction coefficient C_{fx} , the local Nusselt number Nu_x and the local Shearwood number Sh_x as follows:

$$\frac{1}{2} C_{fx} Re_b^{\frac{1}{n+1}} = Af''(0) - [-f''(0)]^n \\ Re_b^{\frac{-1}{n+1}} Nu_x = -\theta'(0) \\ Re_b^{\frac{-1}{n+1}} Sh_x = -\phi'(0) \tag{2.16}$$

III. SOLUTION OF THE PROBLEM

The set of equations (2.10) to (2.12) were reduced to a system of first-order differential equations and solved using a MATLAB boundary value problem solver called **bvp4c**. This program solves boundary value problems for ordinary differential equations of the form $y' = f(x, y, p)$, $a \leq x \leq b$, by implementing a collocation method subject to general nonlinear, two-point boundary conditions $g(y(a), y(b), p)$. Here p is a vector of unknown parameters. Boundary value problems (BVPs) arise in most diverse forms. Just about any BVP can be formulated for solution with **bvp4c**. The first step is to write the ODEs as a system of first order ordinary differential equations. The details of the solution method are presented in Shampine and Kierzenka [33].

IV. RESULTS AND DISCUSSION

The abovementioned numerical scheme is carried out for various values of physical parameters, namely, the material parameter of the Sisko fluid (A), the Brownian motion parameter (Nb), the thermophoresis parameter (Nt), the Prandtl number (Pr), the Lewis number (Le), the thermal Biot number (Bi_1), the concentration Biot number (Bi_2) and the stretching parameter (s) to obtain the effects of those parameters on dimensionless velocity, temperature and concentration distributions. The obtained computational results are presented graphically in Figures 1(a)-12.

In order to validate the method used in this study and to judge the accuracy of the present analysis, comparison with available results of Khan et al. [30] corresponding to the local Nusselt number and local Sherwood number is made (Table 1) and found in excellent agreement and also comparison with available results of Khan et al. [30], Khan and Pop [31], Wang [34] and Gorla and Sidawi [35] corresponding to the local Nusselt number for various values of Pr is made (Table 2) and found in excellent agreement.

The velocity, temperature and concentration distributions for a few values of the power-law index n are demonstrated through Figs 1(a) -3(b). It should be noticed that $n < 1$ relates to shear thinning (pseudoplastic) fluids and $n > 1$ relates to shear thickening (dilatant) fluids. It is anticipated by these figures that the velocity, temperature and concentration distributions diminish as n increases for both shear thinning and shear thickening fluids. This results in a reduction in the momentum, thermal and concentration boundary layers thickness.

Figs 4(a) and 4(b) and 5(a) and 5(b) demonstrate the impact of the Brownian motion parameter Nb and the thermophoresis parameter Nt on the temperature and concentration distributions for the power-law index $n = 1$ and $n = 2$, respectively. Physically, the Brownian motion is stronger in case of smaller nanoparticles which correspond to the larger Nb and converse is the situation for smaller values of Nb . In thermal conduction nanoparticle's motion plays a pivotal role. Due to the intensified chaotic motion of the nanoparticles (i.e., for larger Nb) the kinetic energy of the particles is enhanced which as a result enhances the temperature of the nanofluid. Hence increasing Nb firmly raises temperature values throughout the regime as demonstrated in Fig 4(a) and 4(b). Away from the surface the larger values of Nb stifle the diffusion of the nanoparticles in the fluid regime which reduces the concentration distribution. For higher values of Nb larger thermal boundary layer thickness is formed though larger concentration boundary layer thickness is produced for smaller values of Nb . On the other hand, in nanofluid flow the thermophoresis parameter Nt plays a pivotal role in examining the temperature and nanoparticle concentration distributions. Due to the larger values of Nt the thermophoretic forces are produced. These forces have the tendency to migrate the nanoparticles in the reverse direction of temperature gradient (i.e., from hot to cold) which causes a non-uniform nanoparticle distribution. Consequently, the increasing values of Nt corresponds to an increase in the temperature and nanoparticle concentration distributions as shown in Fig 5(a) and 5(b).

The effect of Prandtl number Pr on temperature and concentration is shown in Figs 6(a) and 6(b) respectively. Physically, enhancing the Prandtl number Pr results in a reduction in thermal diffusivity. It can be seen that the temperature and nanoparticle concentration profiles decrease with an increase in the generalized Prandtl number Pr . This further results in reducing the thermal and concentration boundary layers thickness.

The effect of thermal Biot number Bi_1 and concentration Biot number Bi_2 on temperature and concentration is shown in Figs 7(a) and 7(b), and 8(a) and 8(b) respectively. It is observed that increases the fluid temperature and concentration effectively with increases Bi_1 or Bi_2 . It further increases the thermal and concentration thickness. The effect of thermal radiation R on temperature is shown in Fig 9. It is seen that increases the fluid temperature with the increases R .

Figs 10, 11 and 12 compare the velocity, temperature and concentration profiles of the Newtonian ($A = 0, n = 1$) and the power-law ($A = 0, n \neq 1$) fluid with those of the Sisko ($A \neq 0, n \neq 1$) fluid for the stretching parameter $s = 1.5$ and $s = 2.0$, respectively. Straightforwardly, it is observed the velocity profiles are larger for the Sisko fluid and Newtonian fluid as compared to those of the power-law fluid. But the thermal and nanoparticle concentration profiles are larger for the Newtonian and power-law fluids as compared to those of the Sisko fluid. Additionally, the temperature and concentration boundary layers are highly dependent on the stretching parameters and they diminishes for stronger s .

The effects of material parameter A , the thermophoresis parameter Nt and the Brownian motion parameter Nb on local Nusselt number and local Sherwood number are shown in Figs 13(a) and 13(b), respectively. These figures indicate a decrease in the values of both local Nusselt number and local Sherwood number with the increase in thermophoresis parameter Nt . Further, it can be seen that the effect of the Brownian motion parameter Nb is to decrease the local Nusselt number but its effect is quite opposite on the local Sherwood number and also increase in the values of both local Nusselt number and local Sherwood number with the increase in material parameter A . The effect of thermal Biot number Bi_1 and concentration Biot number Bi_2

on local Nusselt number and local Sherwood number are shown in Figs 14(a) and 14(b), respectively. These figures indicate an increase in the values of local Nusselt number with the increase Bi_1 whereas decrease in the values of local Nusselt number with the increase Bi_2 but its effect is quite opposite on the local Sherwood number.

V. CONCLUSIONS

The two-dimensional steady flow of a Siskonanofluid over a Non-linear stretching sheet in the presence of radiation and convective boundary condition is investigated. Using similaritytransformations, the governing equations are transformed to self-similar ordinary differential equations which are then solved using Bvp4c MATLAB solver. From the study, the followingremarks can be summarized.

1. Fluid temperature increases with an increase thermophoresis parameter, Brownian motion parameter, thermal Biot number, concentration Biot number and thermal radiation parameter.
2. Fluid temperature and concentration decreases with increases the Prandtl number.
3. Fluid concentration increases with an increase thermophoresis parameter, thermal Biot number and concentration Biot number.
4. Fluid concentration decreases with increases the Brownian motion parameter.
5. Local Nusselt number increases with increases the thermal Biot number whereas local Nusselt number decreases with an increase the concentration Biot number.
6. Local Sherwood number increases with increases the concentration Biot number whereas local Sherwood number decreases with an increase the thermal Biot number.

Table 1. Comparison of the present results of local Nusselt number and local Sherwood number for the case of Newtonian fluid for $R=Bi_2=0$ with the results of Khan et al. [30].

A	s	Pr	N_b	N_t	Bi_1	Le	Present Study				Khan et al. [30]			
							$-\frac{-1}{Re_b^{n+1}} Nu_x$		$-\frac{-1}{Re_b^{n+1}} Sh_x$		$-\frac{-1}{Re_b^{n+1}} Nu_x$		$-\frac{-1}{Re_b^{n+1}} Sh_x$	
							n=1	n=2	n=1	n=2	n=1	n=2	n=1	n=2
0	0.5	1	0.1	0.1	0.1	1.5	0.082859	0.088106	0.622438	0.756866	0.082857	0.074467	0.622412	0.715660
0.5	0.5	1	0.1	0.1	0.1	1.5	0.083719	0.083774	0.658043	0.668846	0.083721	0.083772	0.658103	0.668808
1	0.5	1	0.1	0.1	0.1	1.5	0.084197	0.084494	0.679193	0.700421	0.084201	0.084494	0.679343	0.700421
0.5	0.5	1	0.1	0.1	0.1	1.5	0.083719	0.083774	0.658043	0.668846	0.083721	0.083772	0.658103	0.668808
0.5	1	1	0.1	0.1	0.1	1.5	0.085352	0.086843	0.752094	0.864620	0.085352	0.086843	0.752096	0.864615
0.5	2	1	0.1	0.1	0.1	1.5	0.087524	0.089886	0.915235	1.174931	0.087524	0.089886	0.915241	1.174931
0.5	0.5	0.7	0.1	0.1	0.1	1.5	0.080299	0.080079	0.518388	0.517738	0.080291	0.080044	0.518304	0.517209
0.5	0.5	1	0.1	0.1	0.1	1.5	0.083719	0.083774	0.658043	0.668846	0.083721	0.083772	0.658103	0.668808
0.5	0.5	1.3	0.1	0.1	0.1	1.5	0.085840	0.086024	0.777913	0.798377	0.085841	0.086024	0.777992	0.798376
0.5	0.5	1	0.1	0.1	0.1	1.5	0.074470	0.074471	0.701670	0.715667	0.083721	0.083772	0.658103	0.668808
0.5	0.5	1	0.5	0.1	0.1	1.5	0.083719	0.083774	0.658043	0.668846	0.080131	0.080162	0.696729	0.710328
0.5	0.5	1	1	0.1	0.1	1.5	0.080129	0.074470	0.696671	0.701670	0.074472	0.074467	0.701720	0.715660
0.5	0.5	1	0.1	0.1	0.1	1.5	0.083719	0.083774	0.658043	0.668846	0.083721	0.083772	0.658103	0.668808
0.5	0.5	1	0.1	0.5	0.1	1.5	0.083401	0.083467	0.475377	0.470353	0.083402	0.083465	0.475450	0.470141
0.5	0.5	1	0.1	1	0.1	1.5	0.082980	0.083061	0.253794	0.227643	0.082981	0.083059	0.253868	0.227181
0.5	0.5	1	0.1	0.1	0.1	1.5	0.083719	0.083774	0.658043	0.668846	0.083721	0.083772	0.658103	0.668808
0.5	0.5	1	0.1	0.1	0.5	1.5	0.252029	0.252605	0.565377	0.568098	0.252072	0.252584	0.565438	0.567982
0.5	0.5	1	0.1	0.1	1	1.5	0.335699	0.336710	0.519640	0.518123	0.335722	0.336674	0.519698	0.517973
0.5	0.5	1	0.1	0.1	0.1	1.2	0.083782	0.083840	0.564925	0.568468	0.083783	0.083838	0.564987	0.568379
0.5	0.5	1	0.1	0.1	0.1	1.5	0.083719	0.083774	0.658043	0.668846	0.083721	0.083772	0.658103	0.668808
0.5	0.5	1	0.1	0.1	0.1	2	0.083644	0.083695	0.793864	0.814923	0.083645	0.083693	0.793965	0.814913

Table 2. Comparison of the present results of local Nusselt number $-\theta'(0)$ for the case of Newtonian fluid for $N_t=N_b=R=Bi_1=Bi_2=Le=0$ with the results of Khan et al. [30], Khan and Pop [31], Wang [34], and Gorla and Sidawi [35]

Pr	$-\theta'(0)$				
	Present Study	Khan et al. [30]	Khan and Pop [31]	Wang [34]	Gorla and Sidawi [35]
0.7	0.454470	0.45392	0.4539	0.4539	0.5349
2	0.911353	0.91135	0.9113	0.9114	0.9114
7	1.895400	1.89543	1.8954	1.8954	1.8905
20	3.353902	3.35395	3.3539	3.3539	3.3539

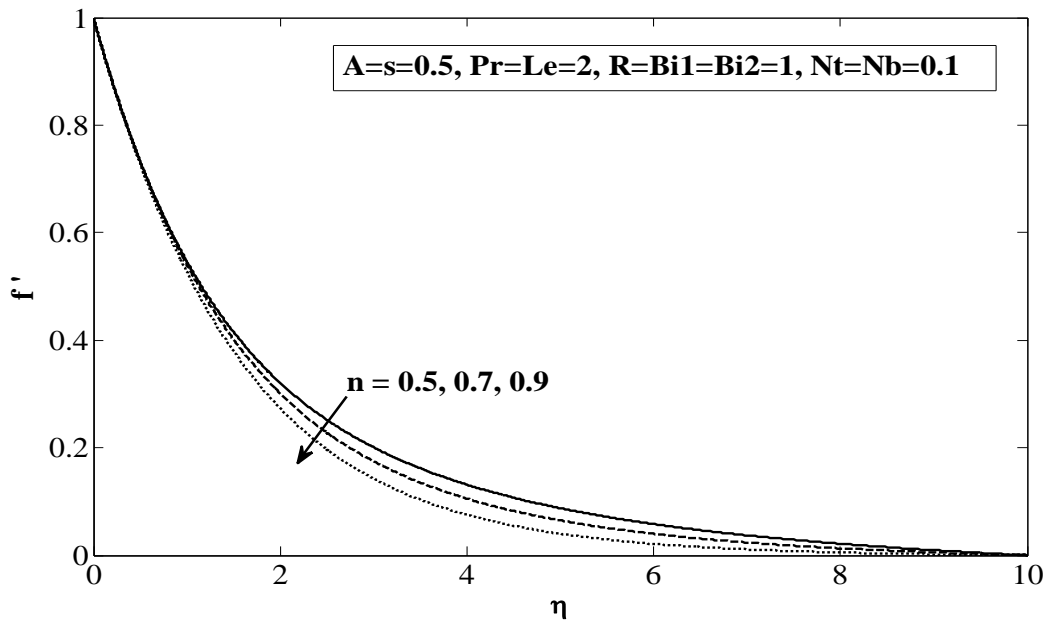


Fig.1 (a) Velocity for different n

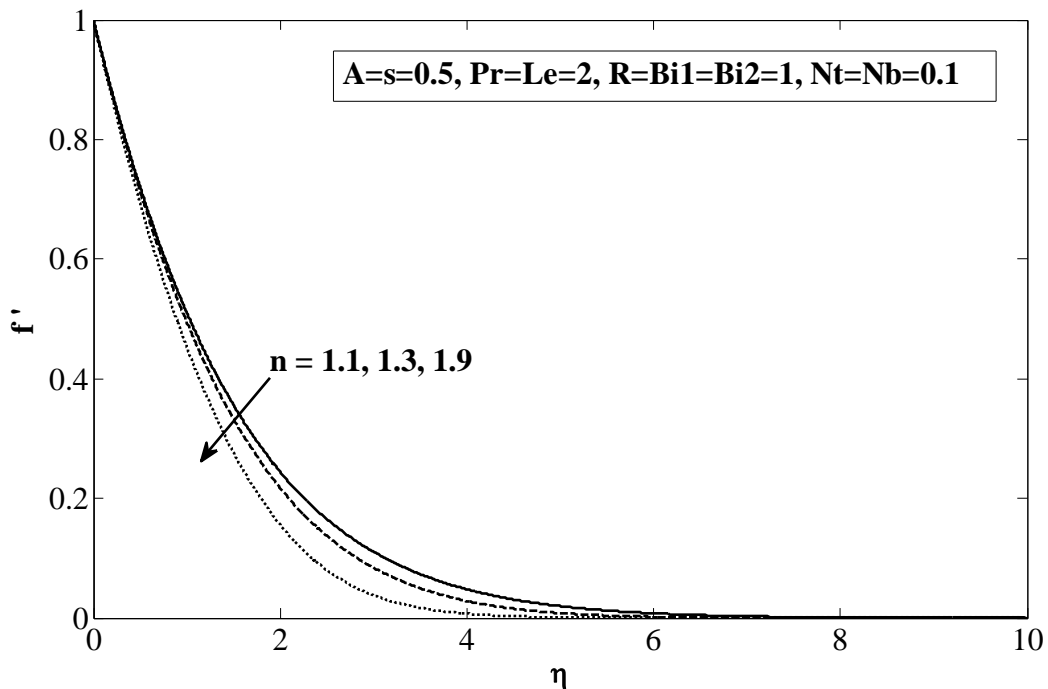


Fig. 1(b) Velocity for different n

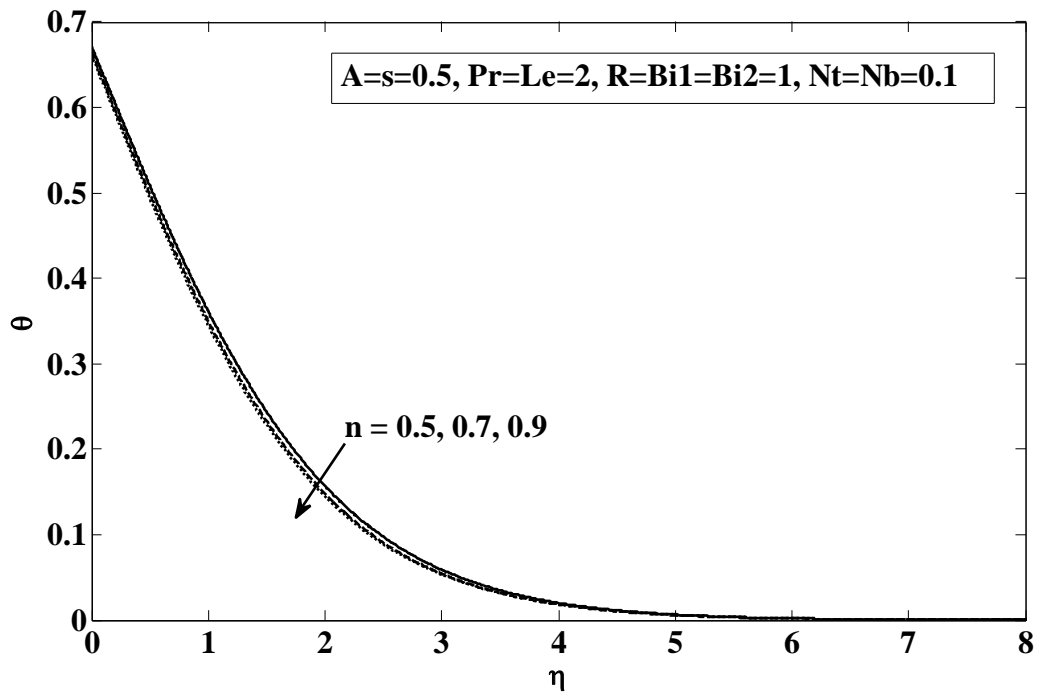


Fig. 2(a) Temperature for different n

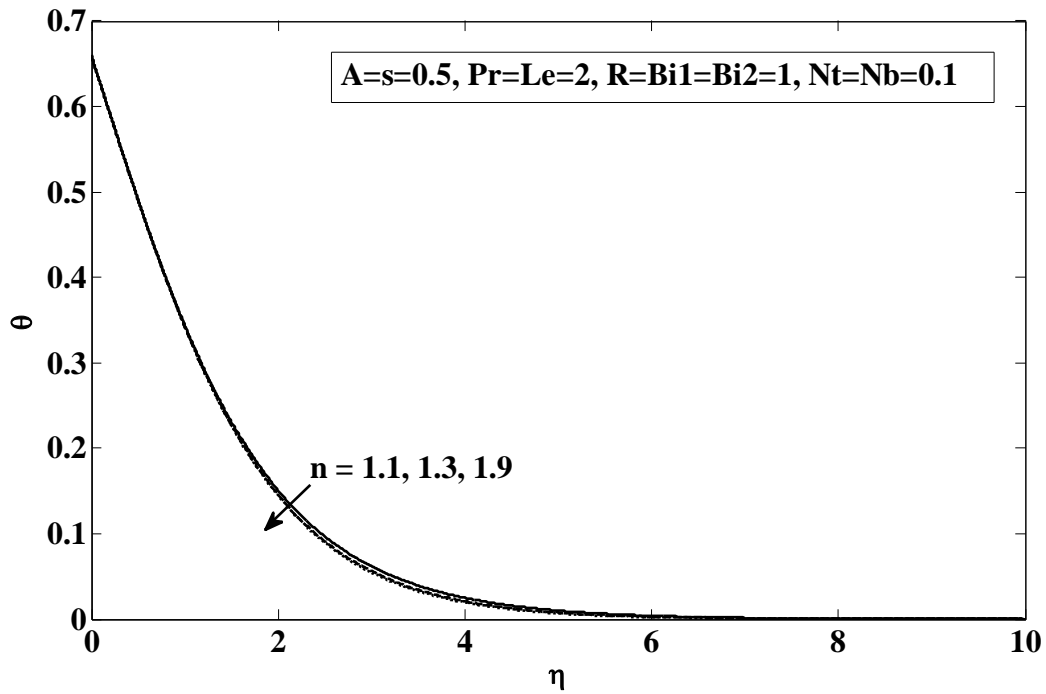
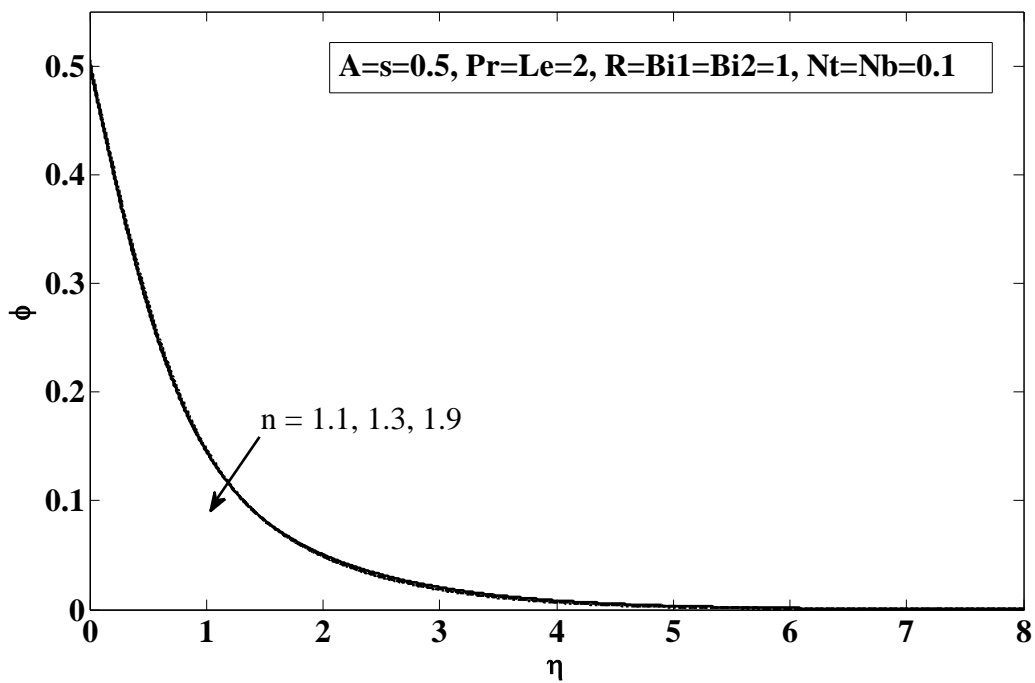
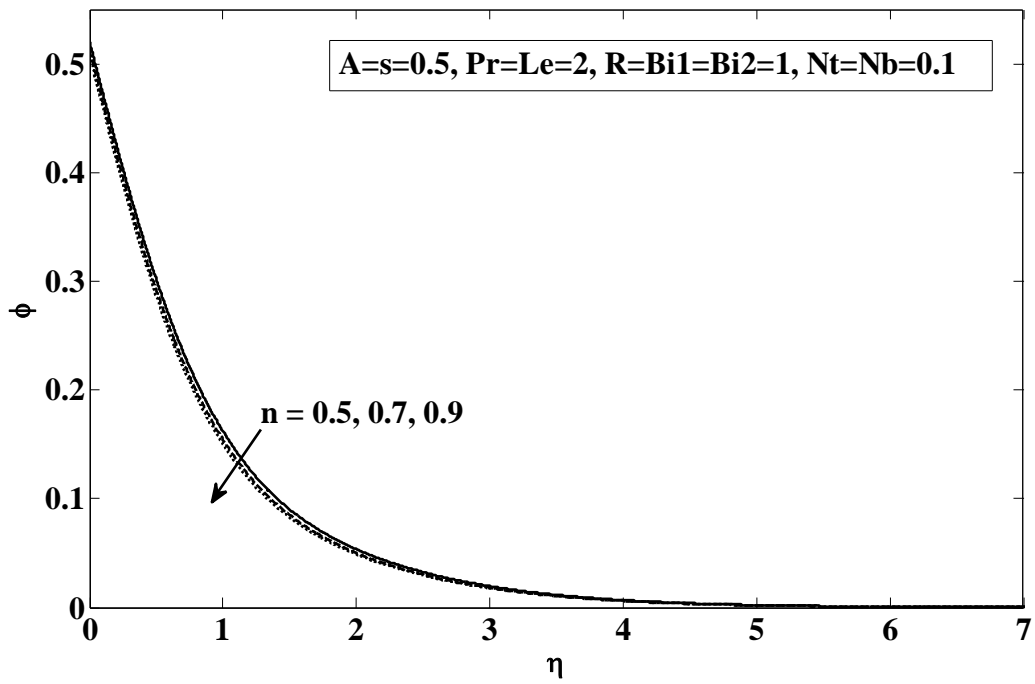


Fig. 2(b) Temperature for different n



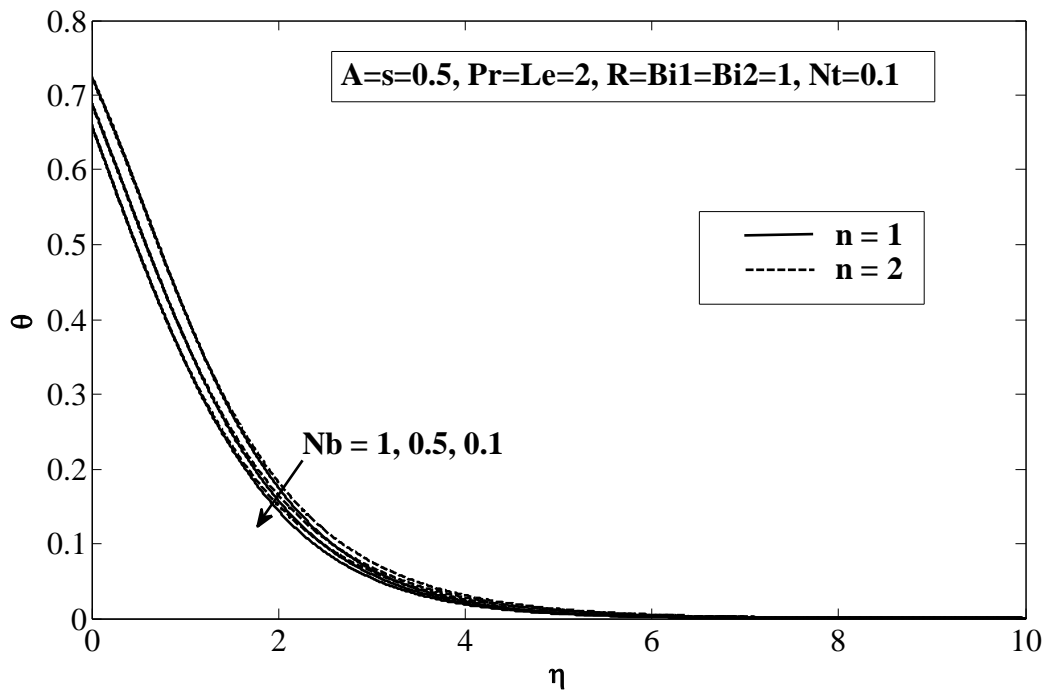


Fig.4(a)Temperature for different Nb

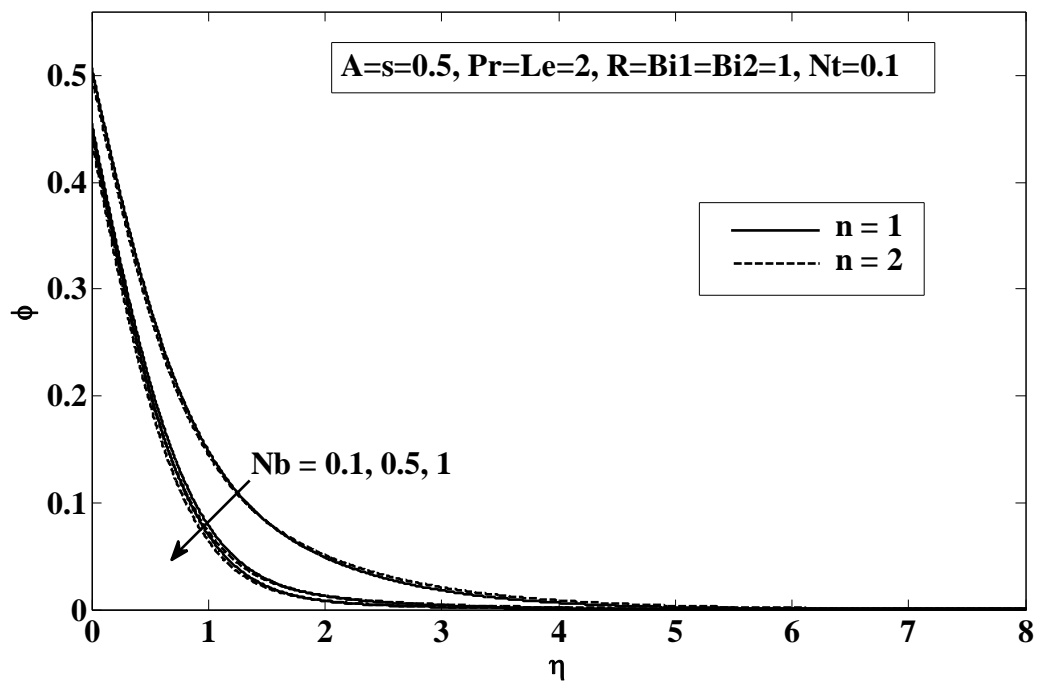


Fig.4 (b)Concentration for different Nb

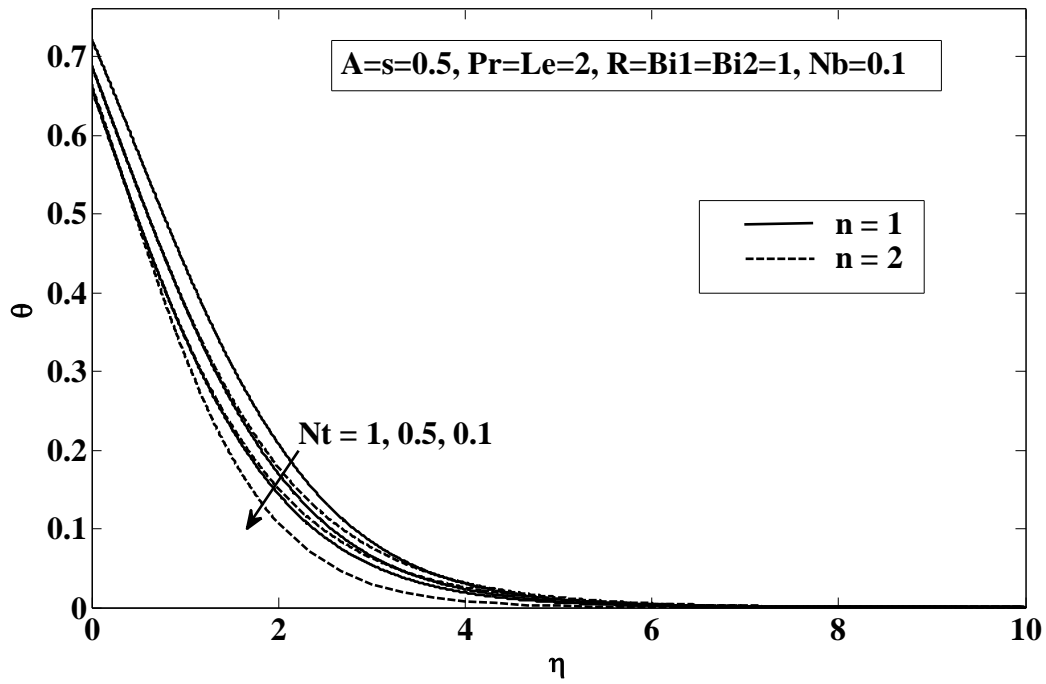


Fig.5 (a) Temperature for different Nt

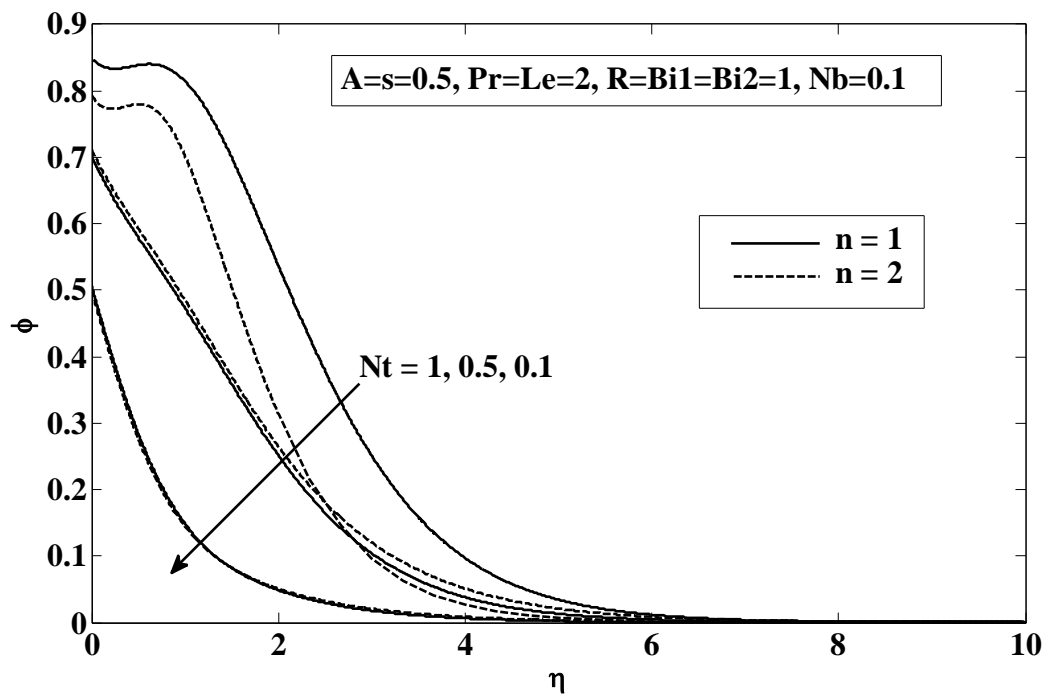
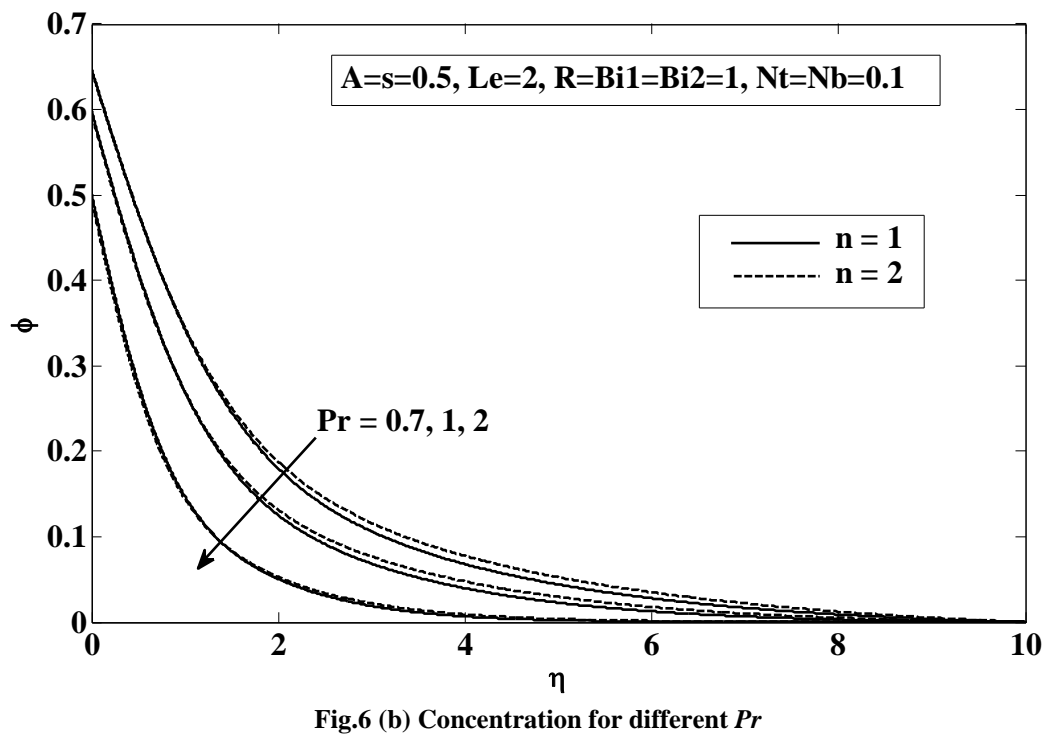
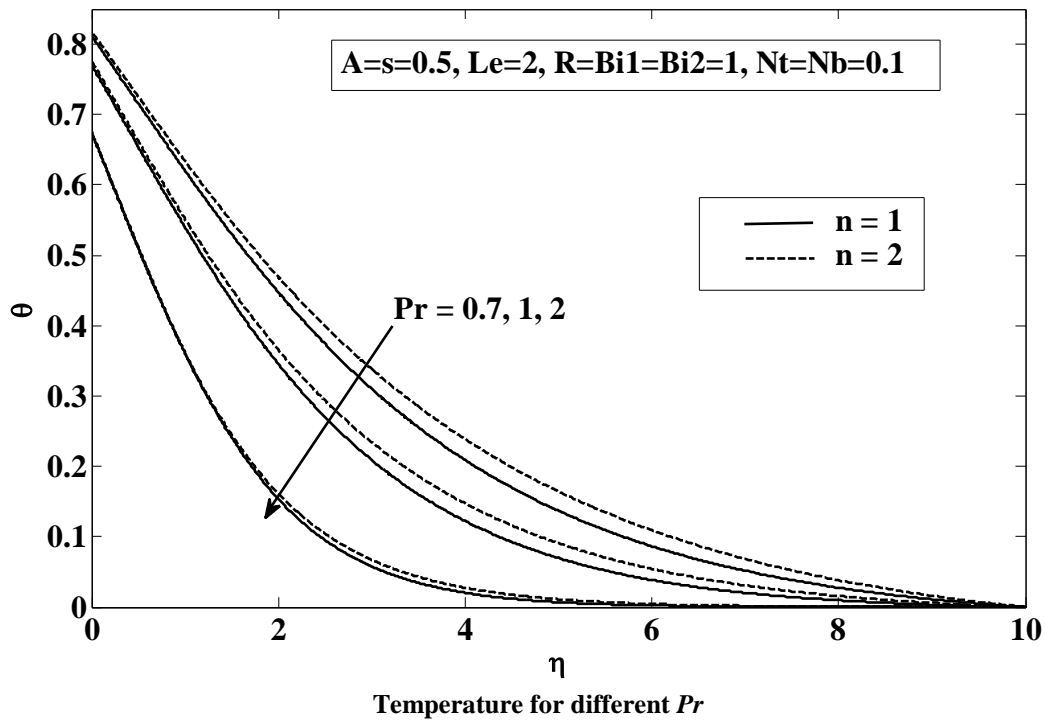


Fig.5 (b) Concentration for different Nt

Fig.6 (a)



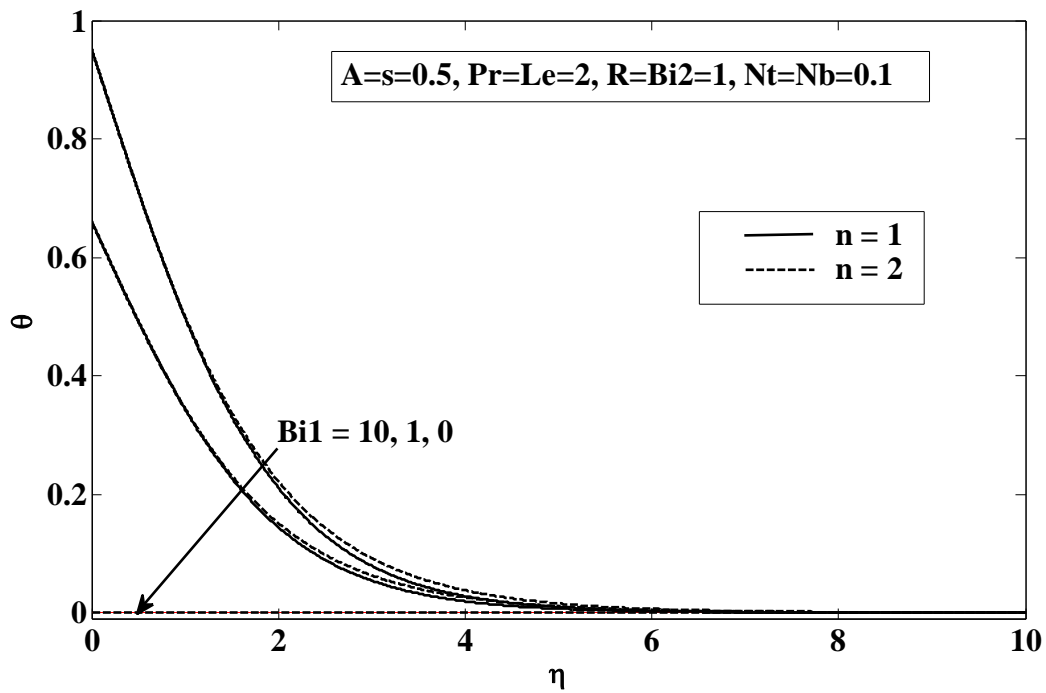


Fig.7 (a) Temperature for different Bi_1

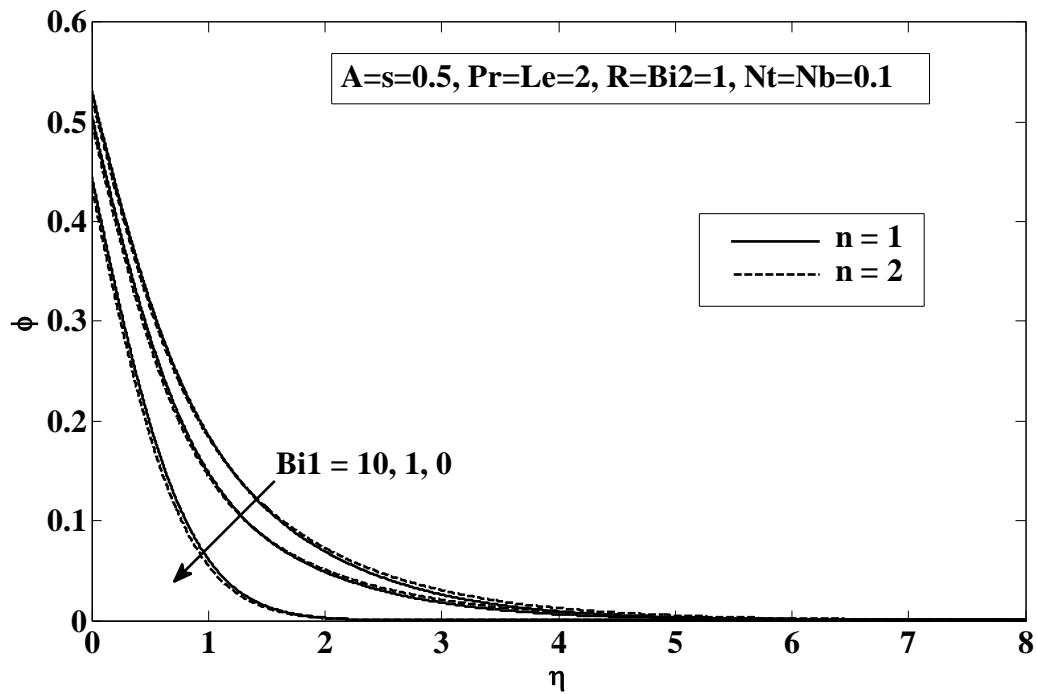


Fig.7 (b) Concentration for different Bi_2

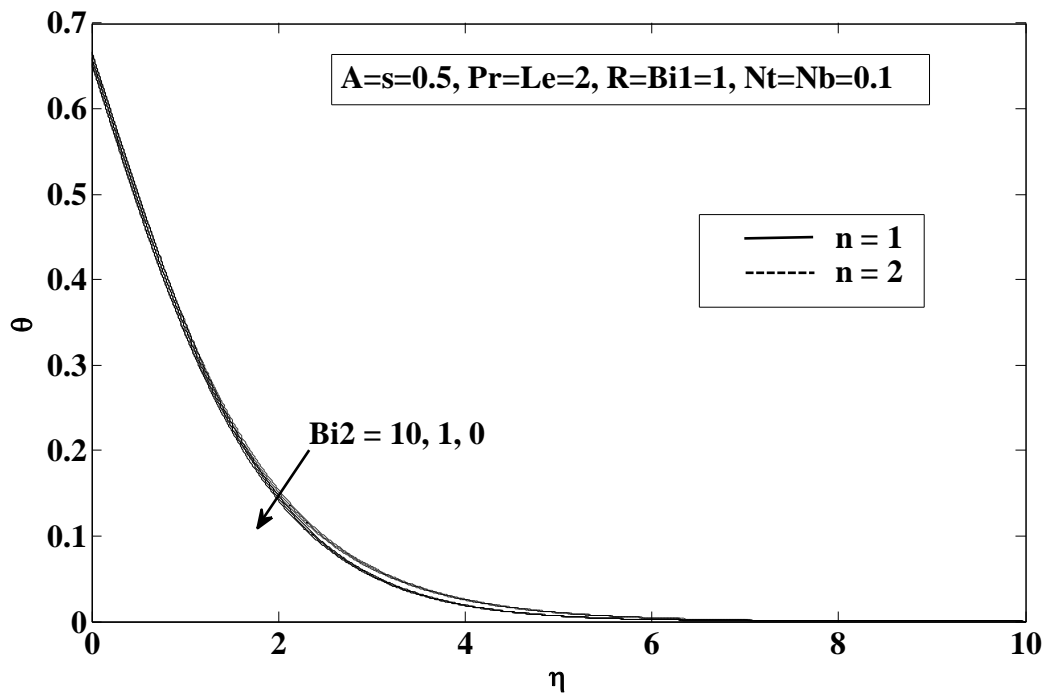


Fig.8 (a) Temperature for different Bi_2

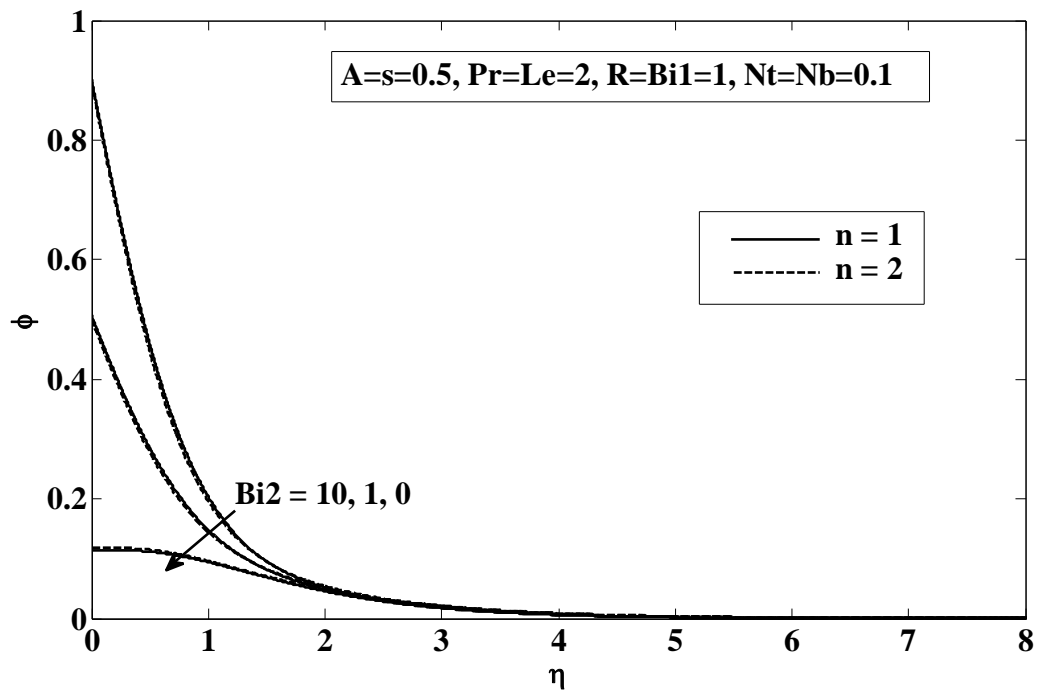


Fig.8 (b) Concentration for different Bi_2

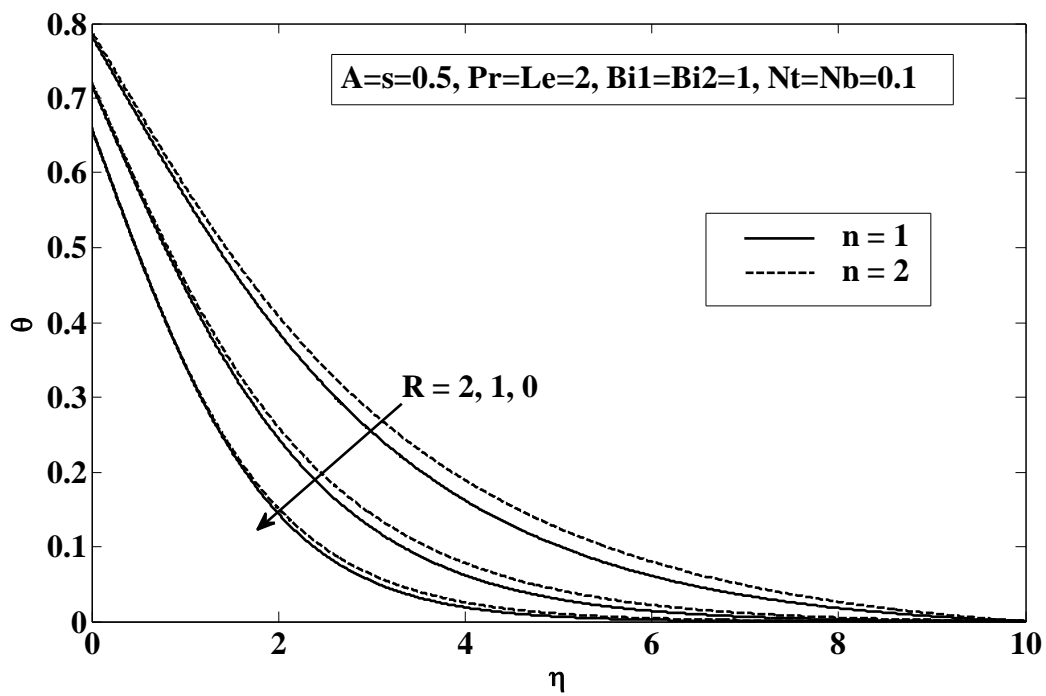


Fig.9 Temperature for different R

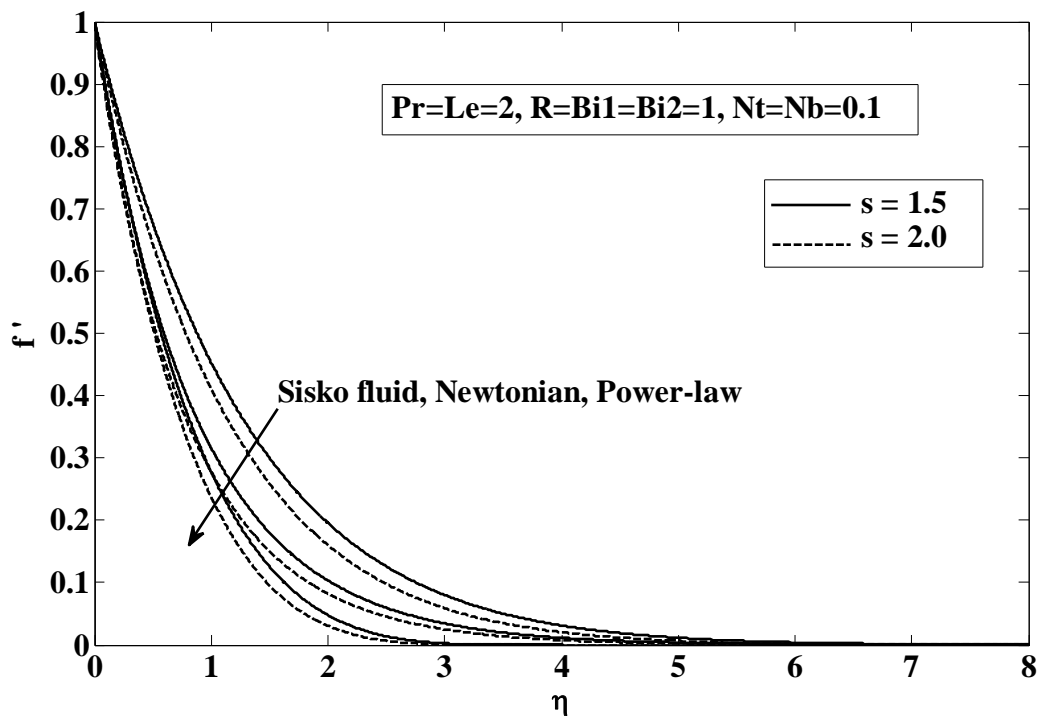


Fig.10 Acomparision of the velocity profiles for Sisko fluid, Newtonian and Power-law fluids.

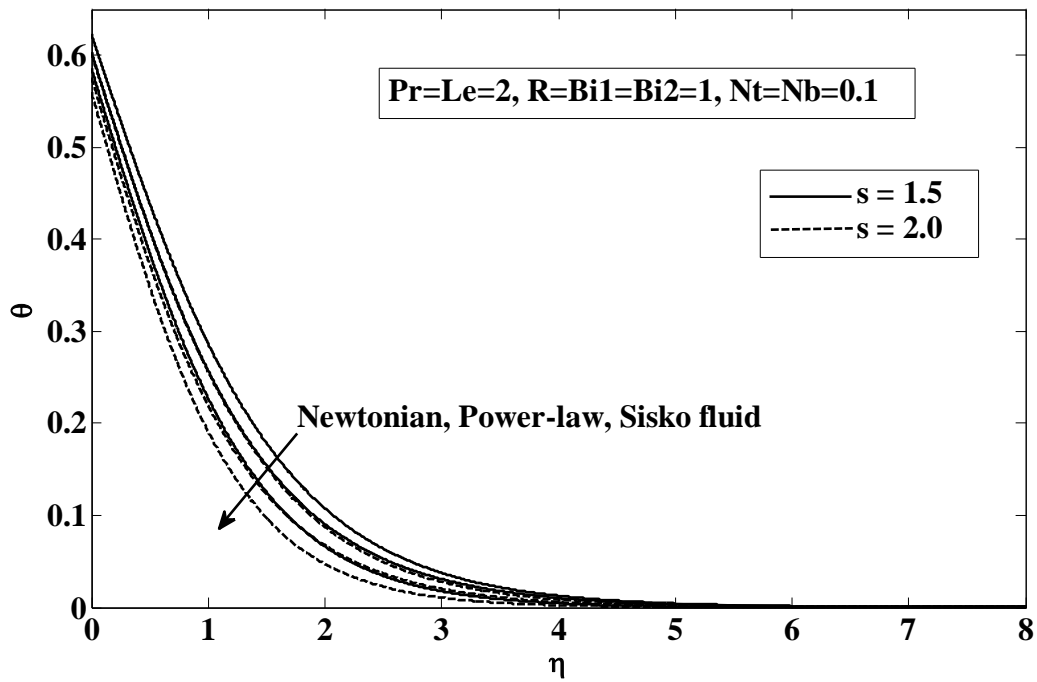


Fig.11A comparison of the Temperature profiles for Newtonian, Power-law and Sisko fluids.

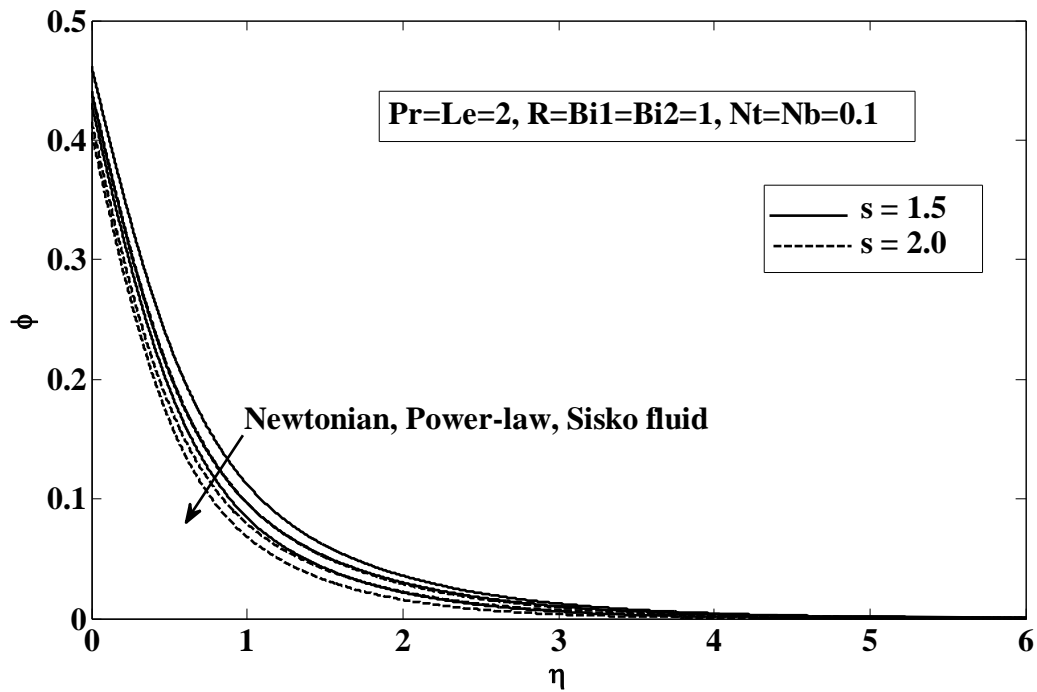


Fig.12A comparison of the Concentration profiles for Newtonian, Power-law and Sisko fluids.

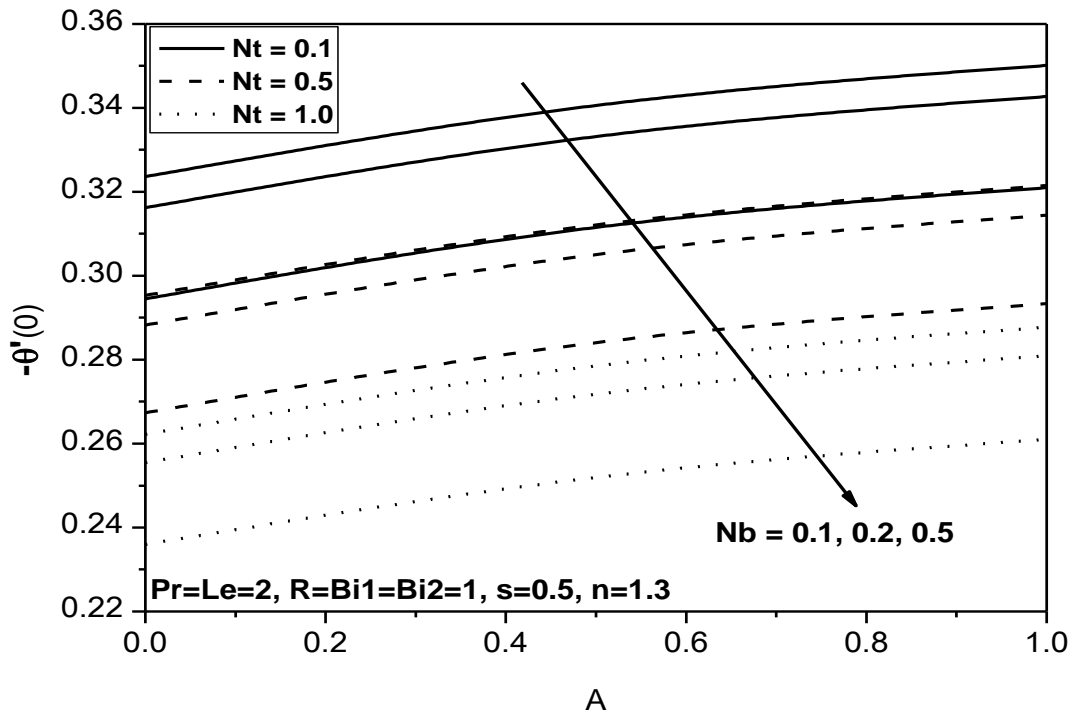


Fig.13 (a) Local Nusselt number for different A , Nt and Nb

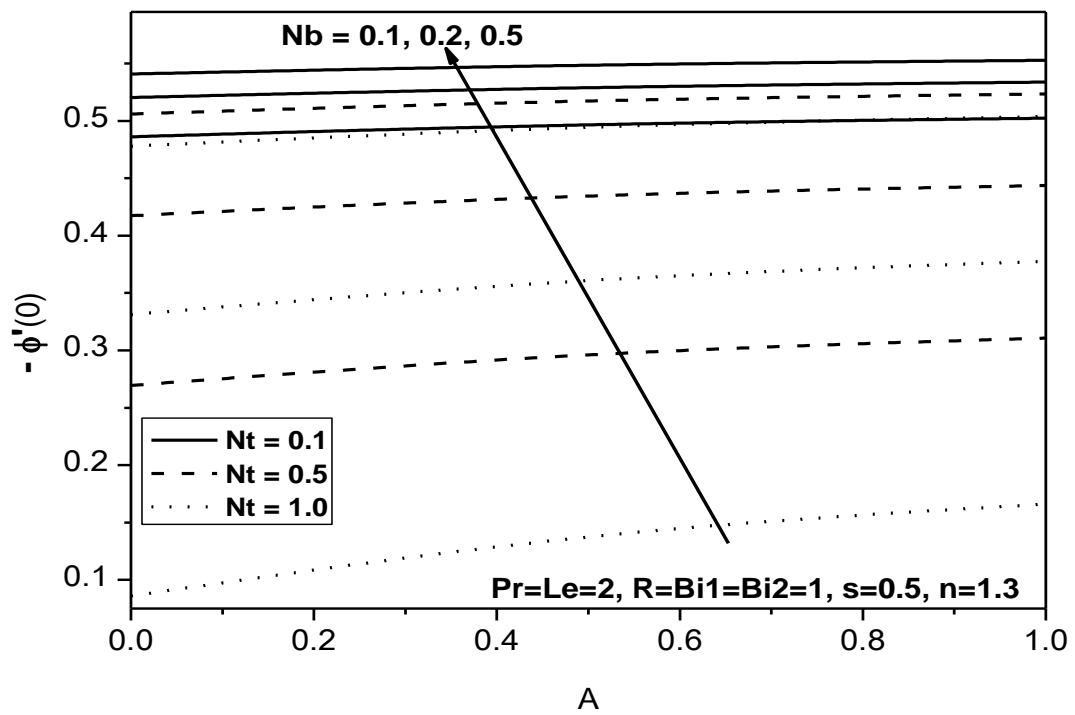


Fig.13 (b) Local Sherwood number for different A , Nt and Nb

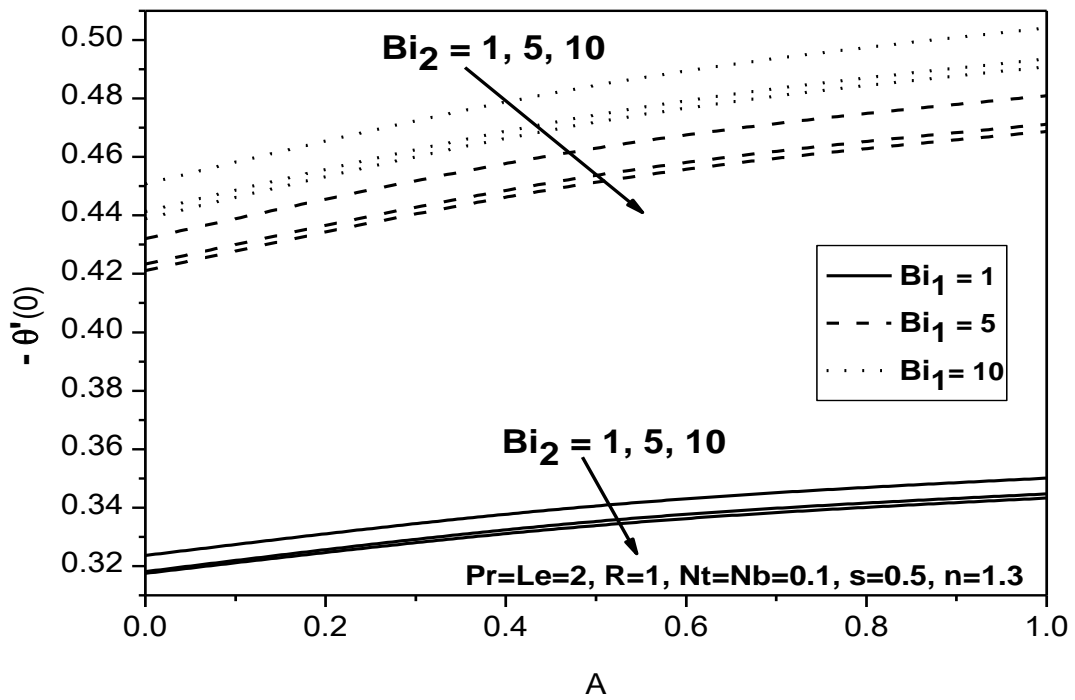


Fig.14 (a) Local Nusselt number for different A, Bi_1 and Bi_2

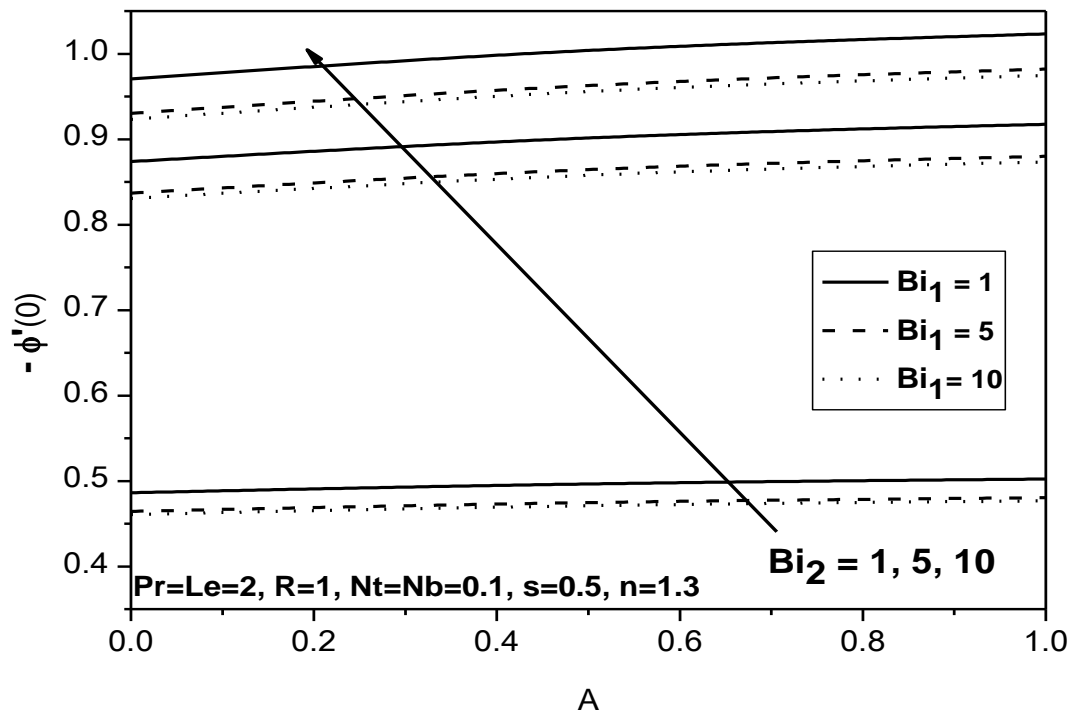


Fig.14 (b) Local Sherwood number for different A, Bi_1 and Bi_2

REFERENCES

- [1]. Nadeem S., Riaz, A., Ellahi, R., and Akbar, N. S., (2014), Effects of heat and mass transfer on peristaltic flow of a nanofluid between eccentric cylinders, *Applied Nanoscience*, vol. 4, pp. 393–404.
- [2]. Zhou, D. W., (2004), Heat transfer enhancement of copper nanofluid with acoustic cavitation, *International Journal of Heat and Mass Transfer*, Vol. 47, no. 14–16, pp. 3109–3117, 2004.
- [3]. Choi, S. U. S., (1995), Enhancing thermal conductivity of fluids with nanoparticles, *ASME Fluids Engineering Division*, Vol. 231, pp. 99–105.
- [4]. Xuan Y. And Li, Q., (2003), Investigation on convective heat transfer and flow features of nanofluids, *Journal of Heat Transfer*, Vol. 125, No. 1, pp. 151–155.
- [5]. Aziz, A., (2009), A similarity solution for laminar thermal boundary layer over a flat plate with a convective surface boundary condition, *Commun. Nonlinear Sci. Numer. Simulat*, Vol.14, pp.1064–1068.
- [6]. Bataller, R.C., (2008), Radiation effects for the Blasius and Sakiadis flows with a convective surface boundary condition, *Appl. Math. Comput.*, Vol.206, Vol.832-840.
- [7]. Ishak, A., (2010), Similarity solutions for flow and heat transfer over a permeable surface with convective boundary condition, *Appl. Math. Computation*, Vol.217, Vol.837-842.
- [8]. Makinde, O.D. and Aziz, A., (2011), Boundary layer flow of a nanofluid past a stretching sheet with a convective boundary condition, *Int. J. Therm. Sci.*, Vol.50, pp.1326-1332.
- [9]. Nor Ashikin Abu Bakar, Wan MohdKhairyAdly Wan Zaimi, Rohana Abdul Hamid, BilianaBidin and AnuarIshak, (2012), Boundary Layer Flow over a Stretching Sheet with a Convective Boundary Condition and Slip Effect, *World Applied Sciences Journal 17 (Special Issue of Applied Math)*, 49-53.
- [10]. Gangadhar, K., (2013), Soret and Dufour Effects on Hydro Magnetic Heat and Mass Transfer over a Vertical Plate with a Convective Surface Boundary Condition and Chemical Reaction, *Journal of Applied Fluid Mechanics*, Vol. 6, No. 1, pp. 95-105.
- [11]. Arpaci, V.S., (1968), Effects of thermal radiation on the laminar free convection from a heated vertical plate, *Int. J. Heat Mass Transfer*, Vol.11, pp.871-881.
- [12]. Cess, R.D., (1966), Interaction of thermal radiation with free convection heat transfer, *Int. J. Heat Mass transfer*, Vol.9, pp.1269-1277.
- [13]. Cheng, E.H and Ozisik, M.N., (1972), Radiation with free convection in an absorbing emitting and scattering medium, *Int. J. Heat Mass Transfer*, Vol.15, pp.1243-1252.
- [14]. Raptis, A., (1998), Radiation and free convection flow through a porous medium, *Int. Comm. Heat Mass Transfer*, Vol.25(2), pp.289-295.
- [15]. Hossain, M.A. and Takhar, H.S., (1996), Radiation effects on mixed convection along a vertical plate with uniform surface temperature, *Heat Mass Transfer*, Vol.31, pp.243-248.
- [16]. Hossain, M.A. and Takhar, H.S., (1999), Thermal radiation effects on the natural convection flow over an isothermal horizontal plate, *Heat Mass Transfer*, Vol.35, pp.321-326.
- [17]. Oahimire, J. I., Olajuwon, B.I., Waheed, M. A., and Abiala, I. O., (2013), Analytical solution to mhdmicropolar fluid flow past a vertical plate in a slip- flow regime in the presence of thermal diffusion and thermal radiation, *Journal of the Nigerian Mathematical Society*, Vol. 32, pp. 33-60.
- [18]. El-Arabawy, H.A.M., (2003), Effect of suction/injection on the flow of a micropolar fluid past a continuously moving plate in the presence of radiation, *Int. J. Heat Mass Transfer*, Vol.46, pp. 1471–1477.
- [19]. Ogulu, A., (2005), On the oscillating plate-temperature flow of a polar fluid past a vertical porous plate in the presence of couple stresses and radiation, *Int. comm. Heat Mass Transfer*, Vol.32, pp. 1231–1243.
- [20]. Nor AzianAini Mat, Norihan M Arifin, RoslindaNazar and Fudziah Ismail, (2012), Radiation effect on Marangoni convection boundary layer flow of a nanofluid, *Mathematical Sciences*, 6:21.
- [21]. MdShakhaoath Khan, IfsanaKarim, MdSirajul Islam and Mohammad Wahiduzzaman, (2014), MHD boundary layer radiative, heat generating and chemical reacting flow past a wedge moving in a nanofluid, *Nano Convergence 2014*, 1:20.
- [22]. MachaMadhu and NaikotiKishan, (2015), Magnetohydrodynamic Mixed Convection Stagnation-Point Flow of a Power-Law Non-Newtonian Nanofluid towards a Stretching Surface with Radiation and Heat Source/Sink, *Hindawi Publishing Corporation Journal of Fluids*, Vol. 2015, Article ID 634186, 14 pages
- [23]. Peri K Kameswaran and Precious Sibanda, (2013), Thermal dispersion effects on convective heat and mass transfer in an Ostwald de Waelenanofluid flow in porous media, *Boundary Value Problems 2013*, 2013:243
- [24]. Nor AzizahYacob&AnuarIsha, (2014), Flow and Heat Transfer of a Power-Law Fluid over a Permeable Shrinking Sheet, *SainsMalaysiana*, Vol.43(3), pp. 491–496.

- [25]. Hayat T., Hussain M., Alsaedi A., Shehzad S. A., and Chen G. Q., (2015), Flow of Power-Law Nanofluid over a Stretching Surface with Newtonian Heating, *Journal of Applied Fluid Mechanics*, Vol. 8, No. 2, pp. 273-280.
- [26]. Kalidas Das , PinakiRanjanDuari, Prabir Kumar Kundu, (2015), Numerical simulation of nanofluid flow with convective boundary condition, *Journal of the Egyptian Mathematical Society*, Vol.23, pp.435–439
- [27]. Hayat T., YusraSaeed, Alsaedi A., SadiaAsad, (2015), Effects of Convective Heat and Mass Transfer in Flow of Powell-Eyring Fluid Past an Exponentially Stretching Sheet, *PLOS ONE*, DOI:10.1371/journal.pone.0133831.
- [28]. Mohammad M. Rashidi, Mohammad Ferdows, Amir BasiriParsa, and Shirley Abelman, (2014), MHD Natural Convection with Convective Surface Boundary Condition over a Flat Plate, *Hindawi Publishing Corporation, Abstract and Applied Analysis*, Volume 2014, Article ID 923487, 10 pages, <http://dx.doi.org/10.1155/2014/923487>
- [29]. Kandasamy R., Jeyabalan C., SivagnanaPrabhu K. K., (2015), Nanoparticle volume fraction with heat and mass transfer on MHD mixed convection flow in a nanofluid in the presence of thermo-diffusion under convective boundary condition, *ApplNanosci*, DOI 10.1007/s13204-015-0435-5.
- [30]. Masood Khan, Rabia Malik, AsifMunir, WaqarAzeem Khan, (2015), Flow and Heat Transfer to SiskoNanofluid over a Nonlinear Stretching Sheet, *PLOS ONE*, DOI:10.1371/journal.pone.0125683, pp.1-13.
- [31]. Khan WA, Pop I., (2010), Boundary-layer flow of a nanofluid past a stretching sheet, *Int J Heat Mass Transf.*, Vol.53, pp.2477–2483.
- [32]. Samir Kumar Nandy, SumantaSidui, Tapas Ray Mahapatra, (2014), Unsteady MHD boundary-layer flow and heat transfer of nanofluid over a permeable shrinking sheet in the presence of thermal radiation, *Alexandria Engineering Journal*, Vol.53, pp.929–937.
- [33]. Shampine, L. F., and Kierzenka, J., (2000), “Solving boundary value problems for ordinary differential equations in MATLAB with bvp4c,” *Tutorial Notes*.
- [34]. Wang C.Y., (1989) Free convection on a vertical stretching surface, *J Appl Math Mech (ZAMM)*, Vol.69, pp. 418– 420.
- [35]. Gorla R.S.R., Sidawi I., (1994), Free convection on a vertical stretching surface with suction and blowing, *ApplSci Res.*, Vol. 52, pp.247–257.